

Implementation of the quantum walk step operator in lateral quantum dots

K. A. van Hoogdalem^{1,2} and M. Blaubaer¹¹ Kavli Institute of Nanoscience, Delft University of Technology,
Lorentzweg 1, 2628 CJ Delft, The Netherlands and² Department of Physics, University of Basel, Klingelbergstrasse 82, CH-4056 Basel, Switzerland
(Dated: February 21, 2024)

We propose a physical implementation of the step operator of the discrete quantum walk for an electron in a one-dimensional chain of quantum dots. The operating principle of the step operator is based on locally enhanced Zeeman splitting and the role of the quantum coin is played by the spin of the electron. We calculate the probability of successful transfer of the electron in the presence of decoherence due to quantum charge fluctuations, modeled as a bosonic bath. We then analyze two mechanisms for creating locally enhanced Zeeman splitting based on, respectively, locally applied electric and magnetic fields and slanting magnetic fields. Our results imply that a success probability of $> 90\%$ is feasible under realistic experimental conditions.

PACS numbers: 73.21.La, 05.40.Fb, 03.65.Yz, 03.67.Lx

The quantum walk (or quantum random walk) is the quantum-mechanical analogue of the classical random walk and describes the random walk behavior of a quantum particle. The concept "quantum walk" was formally introduced by Aharonov et al. in 1993 [1] and suggested earlier by Feynman [2]. The essential difference with the classical random walk lies in the role of the coin: Whereas in the classical random walk the coin is a classical object with two possible measurement outcomes ("heads" or "tails"), in the quantum walk the coin is a quantum-mechanical object—typically a two-level system such as a spin-1/2 particle—which can be measured along different bases and hence has a multi-sided character. As a result, the quantum walk exhibits strikingly different dynamic behavior compared to its classical counterpart due to interference between different possible paths. One example is faster propagation [1]: The root-mean-square distance from the origin $\langle x^2 \rangle_{\text{rms}}$ that is covered by a quantum walker grows linearly with the number of steps N (thus corresponding to ballistic propagation), whereas for the classical random walk $\langle x^2 \rangle_{\text{rms}} \propto \sqrt{N}$ (corresponding to diffusive propagation). This property has been exploited to design new quantum computing algorithms [3]. Both discrete and continuous time quantum walks have been extensively studied in recent years [4], including investigations of decoherence [5] and entanglement between quantum walkers [6].

As far as implementations of quantum walks in actual physical systems are concerned, several proposals have been put forward for a range of optical and atomic systems, such as optical cavities [7], cavity QED systems [8], trapped atoms and ions [9] and linear optical elements [10]. On the experimental side, only a few realizations of quantum walks have been achieved: Discrete and continuous quantum walks in NMR quantum systems [11], discrete quantum walks using linear optical elements [12] and, most recently, a continuous quantum walk in an optical waveguide lattice [13].

For solid-state systems, no realizations of quantum walks exist so far. A recent proposal for implementation of a quantum algorithm using NAND operations in a tree of quantum dots relies on the continuous time quantum walk [14].

In this paper we propose the first implementation of a discrete quantum walk in a solid-state quantum system, which consists of a single electron traveling in a one-dimensional chain of quantum dots. In particular, we focus on the implementation of the so-called step operator, the basic unit of the quantum walk. The step operator causes the electron to either move to the left or to the right depending on the state of the quantum coin, which in our model is represented by the spin of the electron. We calculate the spin-dependent transfer probability of the electron from one dot to the next in the presence of different energy level splittings in neighboring quantum dots (due to locally enhanced Zeeman splitting), taking into account the effects of decoherence due to gate voltage fluctuations [15]. We then propose two physical mechanisms to achieve locally enhanced level splitting in a quantum dot using local electric and magnetic fields and find that under current experimental circumstances successful implementation of the step operator is possible with $> 90\%$ probability.

Model of the step operator.—Consider a chain of three quantum dots in series, in which the middle dot (M) is occupied by a single electron, see Fig. 1. The energy level diagram shows the Zeeman splitting $\epsilon_z^{(0)}$ of the lowest two levels in a magnetic field, and we assume that this splitting is larger in the middle dot by an amount $\frac{0}{z} \epsilon_z$. The gate voltages V_L , V_M and V_R are used to shift the energy levels in the left, middle and right dot resp., and the gate voltages V_T are used to tune the tunnel coupling between neighboring dots. The initial spin state of the electron is a superposition of spin- \uparrow and spin- \downarrow and our first goal is to design an implementation of the step operator such that it causes the electron to

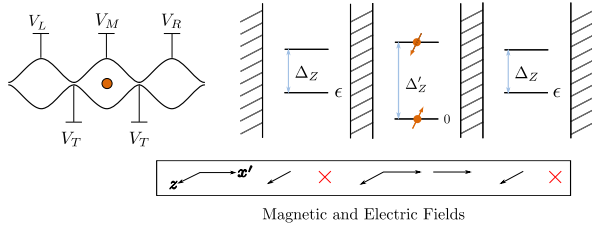


FIG. 1: (left) A linear chain of 3 quantum dots in a magnetic field and (right) the corresponding energy level diagram. The direction of (locally) applied electric and magnetic fields in each dot is also indicated, a cross indicates no applied field. See the text for further explanation.

coherently move to the left (right) if it has spin- \uparrow (spin- \downarrow) and to calculate the probability of successful transfer for this process. To begin with, we assume the right dot to be decoupled from the other two and calculate the spin-dependent probabilities to find the electron in the left and middle dot at a given time. In the absence of decoherence – which is considered further below – the Hamiltonian for the spin- \uparrow and spin- \downarrow components of the electron is given by

$$H_0; = \begin{pmatrix} A & \\ & B \end{pmatrix}; \quad (1)$$

in the basis $\{|\uparrow\rangle; |\downarrow\rangle\}$. Here $(A, B) = (t_L, 0)$, $(A, B) = (t_L + \frac{h}{2}, \frac{h}{2})$ and t_L is the (spin-independent) tunnel coupling between the left and middle dot. The eigenvalues and -vectors of Eq. (1) are given by $E_{\pm} = \frac{A+B}{2} \pm \frac{1}{2} \sqrt{(A-B)^2 + 4t_L^2}$, $j_{+}; i = (\sin \theta; \cos \theta)^T$ and $j_{-}; i = (\cos \theta; \sin \theta)^T$, with $\tan \frac{\theta}{2} = \frac{h}{(A-B)^2 + 4t_L^2}$, $\theta = \theta_L$ and $\theta_{\pm} = (\theta_L \pm \frac{\pi}{2})$. In the absence of decoherence, the solution of the density matrix equations $\dot{\rho} = -i[H_0; \rho]$ for the population in the left dot is given by

$$\rho_{LL}; (t) = \frac{2t_L^2}{(h!)^2} [1 - \cos(\theta_L t)] \quad (2)$$

for initial conditions $\rho_{LL}; (0) = 0$, $\rho_{MM}; (0) = 1$ and $h! = \frac{h}{2} \sqrt{(A-B)^2 + 4t_L^2}$. We see that the probability for the spin- \uparrow component to be in the left dot and the spin- \downarrow component to remain in the middle dot is 1 for $\frac{(h!)^2}{2t_L^2} = 1 - \cos 2n \frac{\theta_L}{\theta_{\pm}}$, $n = 0; 1; 2; \dots$. The smallest n that yields a solution to this equation for $\theta_L = 0$ (zero detuning) is $n = 1$, for which $\theta_L = \frac{\pi}{2}$ and $t = 2\theta_{\pm}$. The second half of the step operator then consists of repeating the same procedure as described above for tunnel coupling between the middle and the right dot, now assuming the left dot to be decoupled.

Decoherence due to quantum fluctuations. – In reality, the time evolution of the occupation probabilities is affected by decoherence due to coupling of the quantum

dots to the environment. In typical experimental situations $k_B T < h!$, for $T = 100$ mK and $1.5 \cdot 10^{-24}$ J [16, 17], so that quantum noise, rather than classical noise, is the dominant source of decoherence. Specifically, since the quantum walk step operator based on the Hamiltonian (1) involves tuning the tunnel couplings – resulting in different charge occupations on neighboring dots – the probability distributions will be strongly affected by fluctuations of charge in the environment [18]. The quantum charge fluctuations we consider here are gate voltage fluctuations, which cause both fluctuations in the tunnel coupling and in the energy levels E of the Hamiltonian (1) [19]. The Hamiltonian which describes the quantum dot system plus the environment is given by

$$H = H_0 + V_A + V_B + H_{\text{bath};} + H_{\text{bath};}; \quad (3)$$

with H_0 the Hamiltonian (1) of the isolated system, $V = \sum_j \hat{c}_j^\dagger \hat{c}_j + \hat{c}_j^\dagger \hat{c}_j$, $V = \sum_j \hat{c}_j^\dagger \hat{c}_j + \hat{c}_j^\dagger \hat{c}_j$, $A = \sum_k \hat{c}_k^\dagger \hat{c}_k + \hat{c}_k^\dagger \hat{c}_k + \hat{b}_k^\dagger \hat{b}_k + \hat{b}_k^\dagger \hat{b}_k$ and $H_{\text{bath};} = \sum_k \hbar \omega_k \hat{b}_k^\dagger \hat{b}_k + \hat{b}_k^\dagger \hat{b}_k + \hat{b}_k^\dagger \hat{b}_k + \hat{b}_k^\dagger \hat{b}_k$. We model the environment as a bosonic bath [20] with creation and annihilation operators \hat{b}_k^\dagger and \hat{b}_k and use the Born-Markov approximation [21] to calculate the time evolution of the spin-dependent occupation probabilities under the Hamiltonian (3), assuming weak coupling between the system and the environment and short correlation times of the boson baths (Markovian assumption). The baths are characterized by the symmetric and anti-symmetric spectral functions $S(\omega)$ with $S^+(\omega) = \coth \frac{\hbar \omega}{2k_B T} S(\omega)$ [20] and we assume Ohmic baths with Lorentzian damping for which $S(\omega) = \hbar^2 \frac{1}{(\omega - \omega_c)^2 + \Gamma^2}$ with ω_c a cut-off frequency. The time evolution of the reduced density matrix $\rho_{ab}(t)$ is then given by $\frac{d\rho_{ab}(t)}{dt} = -i[\rho_{ab}(t), H_0] + \sum_{cd} R_{abcd} \rho_{cd}(t)$, with $R_{abcd} = (E_a - E_b) \delta_{ab} \delta_{cd} + \text{c.c.}$ and R_{abcd} the Bloch-Redfield tensor [20, 22]. Solving this master equation for the two-level system $|\uparrow\rangle; |\downarrow\rangle$ described above for an electron starting at $t = 0$ in the middle dot yields for the evolution of the population of the groundstate $j = \downarrow$ and the coherence term s_{+} :

$$\rho_{jj}; (t) = \frac{1}{2} \left(\tanh \left(\frac{\hbar!}{2k_B T} \right) \cos(2\theta) e^{-\Gamma t} + \frac{\coth \left(\frac{\hbar!}{2k_B T} \right) - 1}{2 \coth \left(\frac{\hbar!}{2k_B T} \right)} \right) \quad (4a)$$

$$s_{+}; (t) = s_{+}; \quad (t) = \sin \theta \cos \theta e^{-\Gamma t} e^{-\Gamma t} \quad (4b)$$

with

$$\Gamma = 4 \frac{t_L^2}{h^2} \cos^2 2\theta + \sin^2 2\theta \coth \frac{\hbar!}{2k_B T} \quad (5a)$$

$$\Gamma = \frac{1}{2} + \frac{8t_L^2}{h^2} \sin^2 2\theta + \cos^2 2\theta k_B T : \quad (5b)$$

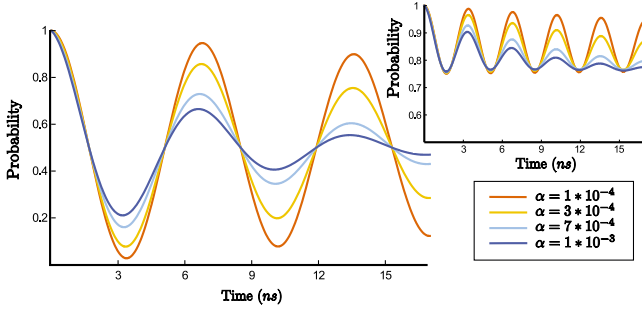


FIG. 2: Survival probability [Eq. (6)] of the spin- \uparrow -component (main plot) and spin- \downarrow -component (inset) in the middle dot as a function of time t for various values of α [23]. Parameters used are $\hbar\omega = 0$, $\hbar\omega_{\#} = 1$ eV, $E = (2 \times 10^3)^{1/2}$ eV [17], and $T = 10$ mK.

Eqs. (4) and (5) are valid in the limit $\omega_{\uparrow}, \omega_{\downarrow} \gg \hbar^{-1} \tau_c$ (with the bath correlation time) [21]. The survival probability to remain in the middle dot at time t is then given by

$$P_{M\uparrow}(t) = \frac{1}{2} [1 + \cos(2\omega_{\uparrow}t) \tanh \frac{\hbar\omega_{\uparrow}}{2k_B T} (1 - e^{-t/\tau_c}) + \cos^2(2\omega_{\uparrow}t) e^{-t/\tau_c} + \sin^2(2\omega_{\uparrow}t) \cos(\omega_{\uparrow}t) e^{-t/\tau_c}] \quad (6)$$

and plotted for both spin- \uparrow and spin- \downarrow in Fig. 2. Using typical experimental parameters (see figure caption and discussion below) we see that successful transfer of the spin- \uparrow component to the left dot while spin- \downarrow remains in the middle dot occurs with probability $> 90\%$ (for $\alpha = 10^{-4}$) at $t = 3.5$ ns.

Locally enhanced Zeeman splitting. – We now consider the question how a different Zeeman splitting in neighboring dots – as assumed in the calculations above – can be realized in practice. In particular, we propose two mechanisms to achieve locally enhanced Zeeman splitting. The first one is by application of a local transverse magnetic field and a local electric field and relies on spin-orbit interaction. Both tunable local magnetic and electric fields have recently been demonstrated experimentally [24, 25]. In our model, see Fig. 1, we assume that a local magnetic field (in addition to the global Zeeman-splitting field B) and a local electric field $E(t)$ are applied to the middle quantum dot. In the presence of spin-orbit interaction, the Hamiltonian for this middle dot is then given by $H = H_0 + eE(t)x + (\frac{\hbar}{2}p_y p_x + \frac{\hbar}{2}p_x p_y)$, with H_0 the Hamiltonian given by Eq. (1), and $\frac{\hbar}{2}p_x p_y$ and $\frac{\hbar}{2}p_y p_x$ the Rashba and Dresselhaus spin-orbit coupling strengths. Using the Schrieffer-Wolff transformation, the Hamiltonian H can be diagonalized to first order in the spin-orbit terms which yields, for the spin-dependent part, $H_{\text{eff}} = \frac{1}{2}g_B B + B(t) \sim 2B$. Here the effective magnetic field B is given by $B = 2B \sim \omega_{\uparrow}(t) + \omega_{\downarrow}(t)$,

with $\omega_{\uparrow}(t) = \frac{e\hbar}{E_z} \omega_{\uparrow}(E_{y^0} = 0; E_{x^0} = 0)$, $\omega_{\downarrow}(t) = \frac{e\hbar}{E_z} \omega_{\downarrow}(E_{x^0} = 0; E_{y^0} = 0)$, $\omega_{\uparrow} = \frac{\hbar}{m} \frac{E_z (E_z^2 - E_1^2) (\hbar\omega_{\uparrow})^2}{(E_z^2 - E_1^2) (E_z^2 - E_2^2)}$, $\omega_{\downarrow} = \frac{\hbar}{m} \frac{E_z^2 \hbar\omega_{\downarrow}}{(E_z^2 - E_1^2) (E_z^2 - E_2^2)}$, $E_z = g_B B$, $E_{1,2} = \hbar \sqrt{4\omega_{\uparrow}^2 + \omega_{\downarrow}^2}$, with $\omega_c = eB/m$ the cyclotron frequency and $m \omega_c^2 r^2 = 2$ the harmonic potential of the quantum dot [27]. In these expressions we have used $x^0 = (x+y)/\sqrt{2}$ and $y^0 = (y-x)/\sqrt{2}$. Since for the step operator we require the eigenstates of the Hamiltonian H to be $|j\rangle$ and $|j\rangle$ we must account for the fact that the eigenvectors of the effective Hamiltonian H_{eff} are transformed by e^S with respect to the eigenvectors of H corresponding to the same eigenvalues. We do this by requiring that the eigenvectors of H_{eff} are $e^S |j\rangle$ and $e^S |j\rangle$ to first order in the action S .

Let us assume the global magnetic field B to be parallel to the z -axis. From the expression for H_{eff} it follows that in order to locally generate a different Zeeman splitting (along the z -axis) in the middle dot compared to its neighboring dots, an additional tunable local magnetic field, e.g. along the x^0 -axis, and a tunable local electric field, also along the x^0 -axis, are required. We define the total (local) magnetic field $B(t) = B_0(n_{x^0}(t); 0; n_z)$. We use the expression for the effective magnetic field combined with the requirement for the eigenvectors of H_{eff} to derive two implicit equations for the magnetic- and electric field in the x^0 -direction as a function of the local magnetic field B in the z -direction:

$$n_{x^0} - n_z \frac{1E_{x^0}}{+} + n_z^2 \frac{1E_{x^0}}{+} = 1 + \frac{B}{B_0} \frac{2c}{1+c^2} \quad (7)$$

$$n_z + n_{x^0} \frac{1E_{x^0}}{+} - n_{x^0} n_z \frac{1E_{x^0}}{+} = 1 + \frac{B}{B_0} \frac{1}{1+c^2} \quad (8)$$

where we have defined $2e\hbar = E_z$ and $c =$

$$\frac{eE_{x^0}}{m \omega_c^2} \frac{1}{+} + \frac{n_{x^0} - 2}{(n_{x^0}^2 + n_z^2) - \frac{1}{+}} y^0.$$

Fig. 3 shows the required fields B_{x^0} and E_{x^0} as a function of B_0 for typical experimental parameters and a local Zeeman splitting of 1 eV [28]. We see that in order to have an additional Zeeman splitting of 1 eV (as assumed in Fig. 2), e.g. at $B_0 = 0.05$ T magnetic and electric fields $B_{x^0} = 63$ mT and $E_{x^0} = 4.6 \times 10^6$ Vm $^{-1}$ are required. Although these values of B_{x^0} and E_{x^0} are (somewhat) larger than those that have been used so far in experiments [24, 30], they may well become available in the near future. Alternatively, one could use larger B_0 (corresponding to larger B_{x^0} and smaller E_{x^0}) or smaller B_z (corresponding to smaller B_{x^0} and E_{x^0} , but also smaller success probability). In addition, we note that in order to preserve the qubit's quantum state, the fields need to be switched on and off adiabatically. The corresponding switching time T of e.g. the tunable magnetic field then has to fulfill [31] $T \geq \frac{\hbar n_{x^0}}{4 n_z \hbar \omega_{\uparrow} \hbar \omega_{\downarrow} B_0} \approx 0.1$ ns. This timescale is well within experimental reach and compat-

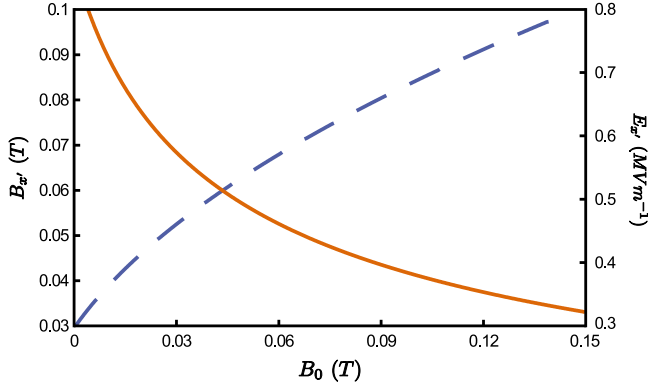


FIG. 3: E_{x0} (solid line) and B_{x0} (dotted line) vs. B_0 for a local magnetic field B corresponding to a Zeeman splitting of 1 eV. Parameters used are $\hbar\omega_0 = 1$ meV [27], $m = 0.067m_e$ (for GaAs [27]), $\mu_B = 2$ m, $\mu_D = 10$ m [24, 29], and $n_z = 1$.

able with the operation time (duration of electron transfer) ~ 3.5 ns that we estimated above.

Another method to generate different Zeeman fields in neighboring dots is by using a slanting magnetic field. The latter has recently been demonstrated for the first time by integrating a microsize ferromagnet in a double dot device [32]. As a result of the slanting field, the orbital and spin degrees of freedom become hybridized, leading to an effective mixed charge-spin two-level system, where the role of the coin is played by the pseudospin instead of the real spin. A global magnetic field 2 T magnetizes the ferromagnet and its inhomogeneity leads to a different Zeeman field in the two quantum dots of $B_z \sim 10$ mT ($j_z = \frac{0}{2}j = 4 \cdot 10^6$ J [32]). An advantage of this method compared to using spin-orbit interaction (as discussed above) is that no tunable magnetic fields but only tunable gate voltages are needed. A disadvantage is that the qubit is likely to be more sensitive to orbital decoherence.

Finally, we briefly discuss the question of how to extend our model from 3 quantum dots to a longer one-dimensional chain. In order for the electron to perform a quantum walk along the chain, opening and closing of tunnel barriers and aligning energy levels has to be applied at every position where the particle has a finite probability of being found. In addition, not only a step operator, but also a reinitialization operator C of the coin (spin) degree of freedom is needed [1]. A common choice for C is the Hadamard operator [4], which can be implemented by two coherent rotations around different axes [24, 25, 33]. The dynamics of a quantum walk of electrons along a one-dimensional chain of quantum dots in the presence of decoherence remains an interesting question for future research.

In conclusion, we have proposed an implementation of a discrete quantum walk step operator in a solid-state nanostructure consisting of a linear chain of 3 quantum

dots. For currently available techniques to locally create enhanced Zeeman splitting and taking into account decoherence due to quantum charge fluctuations, we have analyzed the probability for coherent transfer of the electron to the left or right (conditioned on its spin), and predict that $> 90\%$ success probability is feasible. We hope that our results will stimulate a proof-of-principle experimental demonstration of the discrete quantum walk step operator in a solid-state nanosystem.

This work has been supported by the Netherlands Organisation for Scientific Research (NWO).

-
- [1] Y. Aharonov, L. Davidovich, and N. Zagury, *Phys. Rev. A* **48**, 1687 (1993).
 - [2] R. P. Feynman and A. R. Hibbs, *Quantum mechanics and path integrals*, (McGraw-Hill, New York, 1965).
 - [3] V. Kendon, *Phil. Trans. R. Soc. A* **364**, 3407 (2006).
 - [4] Two recent reviews on quantum walks are J. Kempe, *Contemp. Phys.* **44**, 307 (2003) and V. Kendon, *Math. Struct. in Comp. Sci.* **17**, 1169 (2007).
 - [5] T. A. Brun, H. A. Carteret, and A. Ambainis, *Phys. Rev. Lett.* **91**, 130602 (2003); A. Romanelli et al., *Physica A* **347**, 137 (2005); L. Ermann, J. P. Paz, and M. Saraceno, *Phys. Rev. A* **73**, 012302 (2006); N. V. Prokofev and P. C. E. Stamp, *ibid.* **74**, 020102 (2006); J. Kosik, V. Buzek, and M. Hillery, *ibid.*, 022310 (2006); A. P. Hines and P. C. E. Stamp, *Can. J. Phys.* **86**, 541 (2008).
 - [6] S. E. Venegas-Andraca et al., *New J. Phys.* **7**, 221 (2005); G. A. Balle et al., *Phys. Rev. A* **73**, 042302 (2006); Y. Omar et al., *ibid.* **74**, 042304 (2006).
 - [7] P. L. Knight, E. Roldan, and J. E. Sipe, *Opt. Comm.* **227**, 147 (2003);
 - [8] B. C. Sanders et al., *Phys. Rev. A* **67**, 042305 (2003); G. S. Agarwal and P. K. Pathak, *ibid.* **72**, 033815 (2005).
 - [9] B. C. Travaglione and G. J. Milburn, *Phys. Rev. A* **65**, 032310 (2002); W. Dur et al., *ibid.* **66**, 052319 (2002); K. Eckert et al., *ibid.* **72**, 012327 (2005); Z.-Y. Ma et al., *ibid.* **73**, 013401 (2006).
 - [10] P. K. Pathak and G. S. Agarwal, *Phys. Rev. A* **75**, 032351 (2007).
 - [11] J. Du et al., *Phys. Rev. A* **67**, 042316 (2003); C. A. Ryan et al., *ibid.* **72**, 062317 (2005).
 - [12] B. Do et al., *J. Opt. Soc. Am. B* **22**, 499 (2005); P. Zhang et al., *Phys. Rev. A* **75**, 052310 (2007).
 - [13] H. B. Perets et al., *Phys. Rev. Lett.* **100**, 170506 (2008).
 - [14] J. M. Taylor, arXiv:0708.1484v1 [quant-ph]
 - [15] In Ref. [14] the effects of dephasing are taken into account in a phenomenological way and modeled by a dephasing rate γ .
 - [16] See e.g. J. R. Petta et al., *Science* **309**, 2180 (2005).
 - [17] F. H. L. Koppens et al., *Science* **309**, 1346 (2005).
 - [18] Fluctuations in the nuclear spin environment, which is coupled to the electron spin via the hyperfine interaction, are slow (typically of the order of microseconds or more, see e.g. J. M. Taylor et al., *Phys. Rev. B* **76**, 035315 (2007)). The nuclear field therefore acts as a frozen external field during the step operation and we neglect its fluctuations in our model.
 - [19] A. Romanito and Y. Gefen, *Phys. Rev. B* **76**, 195318 (2007).

- [20] U. Weiss, *Quantum dissipative systems*, (World Scientific, Singapore, 1999).
- [21] C. Cohen-Tannoudji, J. Dupont-Roc, and G. Grynberg, *Atom-photon interactions*, (Wiley, New York, 1998).
- [22] The sum extends over terms with $|\alpha_b\rangle \langle \alpha_d| = 1 = t$ (secular constraint) where t is the timescale of the Markovian coarse-grained evolution [21].
- [23] Values of γ in this range were measured by O. Astaev et al., *Phys. Rev. Lett.* 93, 267007 (2004).
- [24] K. C. Nowack et al., *Science* 318, 1430 (2007).
- [25] F. H. L. Koppens et al., *Nature* 442, 766 (2006).
- [26] M. Borhani, V. N. Golovach, and D. Loss, *Phys. Rev. B* 73, 155311 (2006); V. N. Golovach, M. Borhani, and D. Loss, *ibid.* 74, 165319 (2006).
- [27] For a recent review on spin qubits in quantum dots see R. Hanson et al., *Rev. Mod. Phys.* 79, 1217 (2007).
- [28] Similar values for B_{x^0} and E_{x^0} are found for an in-plane global magnetic field and out-of-plane local fields.
- [29] J. B. Miller et al., *Phys. Rev. Lett.* 90, 076807 (2003); S. Amasha et al., *ibid.* 100, 046803 (2008).
- [30] E. A. Laird et al., *Phys. Rev. Lett.* 99, 246601 (2007).
- [31] A. Messiah, *Quantum Mechanics*, (Dover, 1999), Ch. XV II.
- [32] M. P. Pioro-Ladriere et al., *Nature physics* 4, 776 (2008); Y. Tokura et al., *Phys. Rev. Lett.* 96, 047202 (2006).
- [33] M. Nielsen and I. Chuang, *Quantum Computation and Quantum Information*, (Cambridge University Press, Cambridge, 2000).